

Synthesis and Electrical Properties of Polyacetylene Copolymers from Poly(phenyl vinyl sulfoxide) and Its Oxidized Products

Louis M. Leung* and Kam Ho Tan

Department of Chemistry, Hong Kong Baptist College, 224 Waterloo Road, Kowloon, Hong Kong

Received November 13, 1992; Revised Manuscript Received May 20, 1993

ABSTRACT: Poly(phenyl vinyl sulfoxide), a soluble precursor to polyacetylene, was synthesized by anionic polymerization. Different fractions of the thermally labile phenyl vinyl sulfoxide pendant groups were oxidized to thermally stable phenyl vinyl sulfones in order to control the degree of conjugation in the polymer main chain after elimination. The mean conjugation length (MCL), the total number percentage of nonconjugated structures or nonconductive defects, and the weight and volume fractions of acetylene units in the eliminated copolymers were calculated and correlated with their bulk conductivities after doping with iodine. A sigmoidal dependence on conductivity and a maximum in the dissipation factor measurement were observed for the four calculated variables over the full composition range. Compared to the effective-medium theory for a conducting composite, the transition range is rather broad and the "percolation" threshold at about 35–38% by volume of acetylene is equivalent to a MCL of 3 and 25% defects.

Introduction

Organic conducting polymers have been one of the focuses of polymer research in the past decades.^{1,2} The application of conducting polymers, however, is still very much limited. This is due to conjugated polymers in general being difficult to process and having low thermal and environmental stability, especially after doping. Their electrical conductivities are also less than desirable when compared to those of metals and alloys. The conductivity of a saturation doped conducting polymer normally is in the range of 10^1 to 10^3 S/cm before orientation or stretching. This is considerably less conductive than metallic conductors like copper, which has a conductivity in the range of 10^6 S/cm and the capability of carrying a larger current density. These are some of the drawbacks that restricted conducting polymers from replacing metals in a wide range of electrical applications. Yet conjugated polymers possess novel and special properties that are essentially different from metals, such as their low relative densities, semi-conducting and nonlinear optical characteristics, etc. Thus conducting polymers have promising new applications like lightweight rechargeable batteries, molecular size micro-electronic and photonic devices or sensors, etc. Besides metal-like conductivity, there has also been a demand for materials with a range of resistivity and permittivity for electronic and electrical applications.

The mechanism of charge transport in a polymeric conductor is still not very well understood. A high degree of conjugation is suggested to be a prerequisite for high conductivity due to the availability of delocalized π -electrons. Mechanisms such as hopping, tunneling, and band gap theory have been proposed. A further complication to the situation has been due to experimentally measured bulk conductivity usually being a combination of intra-chain, interchain, and interparticle (or interdomain) charge transport processes. A recent study by Thakur³ has shown that a nonconjugated polymer also has a manifolded increase in conductivity upon doping. The phenomenon was suggested to be a result of formation of conducting complexes in the presence of electron-releasing substituents. In the past, polyacetylene with different substituents has been synthesized but no significant or systematic

changes in electrical properties have been reported.^{1,4} The substituted groups affected also both the stability and the morphology (such as crystallinity) of the conducting polymer. It is therefore difficult to establish a relationship between the nature of the substituent and the intrinsic conductivity of the polymer chain. By control of the degree of elimination in a conducting precursor, however, the degree of conjugation can be readily correlated with the electrical properties of the resulting conducting polymer.

Polyacetylene (PA) has been the most studied conducting polymer since its chemical structure is simple and its synthesis is relatively easy.⁴ In the Shirakawa method,⁵ Ziegler–Natta catalyst was used to produce an infusible polyacetylene film with fibrillar structure. To improve on its processability, soluble precursors^{6,7} as well as block or graft copolymers of polyacetylene^{8,9} have been prepared. Recently, a series of papers by Kanga and Hogen-Esch et al.^{10,11} has demonstrated the feasibility of synthesizing poly(phenyl vinyl sulfoxide) via an anionic polymerization technique. The result is an organic solvent-soluble PA precursor with known and narrow molecular weight distribution.

In this study, electrical properties of a series of PA resulting from the elimination of poly(phenyl vinyl sulfoxide) and its copolymers are reported. In order to establish a correlation between the degree of conjugation in the polymer's backbone structure and its electrical properties, the anionic prepared polymers were oxidized randomly to convert the thermally labile phenyl vinyl sulfoxide pendant groups to thermally stable phenyl vinyl sulfone moieties. The copolymers then underwent thermal elimination to produce a series of acetylene–phenyl vinyl sulfone copolymers with different mean conjugation lengths. The mean conjugation length, the volume and weight fractions of the acetylene units, and the total number of nonconductive defects in the copolymers were all calculated in order to establish their relationships with the bulk electrical properties measured. The applicability of Bruggeman's effective-medium theory for a conducting composite is also investigated for this conducting copolymer system.¹²

Experimental Section

Phenyl vinyl sulfide (VS), phenyl vinyl sulfoxide (VSO), and phenyl vinyl sulfone (VSO₂) were prepared according to the synthetic routes suggested by Paquette¹³ with some modifications.

* To whom all correspondence should be addressed. Phone: 852-339-7073. Fax: 852-338-8014.

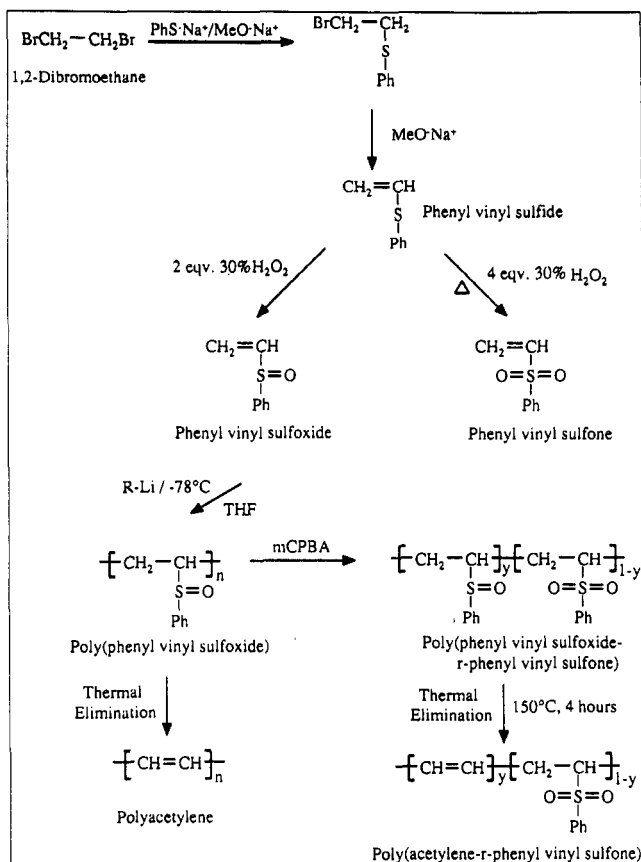


Figure 1. Synthetic routes for the monomers and conducting copolymer precursor.

A summary of the reactions that leads to the formation of the monomers and the resulting copolymers is given in Figure 1. All chemicals and solvents used were reagent grade unless otherwise specified.

Synthesis of the Monomer. Thiophenol (Fluka) (50 mmol) was added slowly to a 15% sodium methoxide solution at room temperature. The resulting sodium thiophenoxide solution was added dropwise to a solution containing 75 mmol of 1,2-dibromoethane and methanol under constant stirring. At the end of the addition, an equal portion of 15% sodium methoxide was poured into the reaction mixture. The solution was then refluxed for 8 h. Water was added to the final mixture at room temperature, and methylene chloride (MeCl) was used to extract VS from the aqueous phase. The product VS was purified by vacuum distillation ($40\text{--}45^\circ\text{C}$, 1 mmHg). The yield for VS was about 72%. The major side product for this reaction was 1,2-bis(phenylthio)ethane and its yield can be further reduced by raising the molar ratio of 1,2-dibromoethane.

VS was oxidized to VSO in acetic acid by a 2 molar excess of 30% hydrogen peroxide added dropwise. The mixture was allowed to react for 24 h at room temperature. The product VSO was collected by extraction from the aqueous phase using MeCl . VSO was further purified by vacuum distillation (92°C , 0.2 mmHg) over calcium hydride. The yield was 80%, and the loss was mostly due to VSO decomposition during distillation. VSO_2 was obtained by oxidation of VS in acetic acid using an excess of 4 M 30% hydrogen peroxide added dropwise. The mixture was then heated to 110°C for 1 h. The product was again extracted from the aqueous phase using MeCl . VSO_2 was collected and purified by recrystallization in *n*-hexane. After drying under vacuum, the yield was 89%. The chemical composition and purity for each of the reaction products were determined by IR spectrometry and $^1\text{H-NMR}$.

Anionic Polymerization. Five different lithium anionic initiators were used for the polymerization of VSO. A 1.6 M *n*-butyllithium (*n*-BuLi) in *n*-hexane solution was purchased (Fluka) and used "as received". Other lithium initiators, all at approximately 1 M, were prepared in this lab using lithium metal and their parent compounds in dried tetrahydrofuran (THF).

The initiators were "packed" under dried nitrogen in an ultrasonic bath at room temperature. Two alkyl lithium initiators (*n*-butyllithium (*n*-BuLi) and phenyllithium (PhLi) prepared from purified bromobenzene), one electron-transfer initiator (lithium naphthalide (LiNaph) from purified naphthalene), and two delocalized carbanions ((diphenylmethyl)lithium (DPMLi) from purified diphenylmethyl chloride and (triphenylmethyl)lithium (TPMLi) from triphenylmethyl chloride) were used for the anionic reaction. The molar concentration of the initiators was determined using the Gilman titration method¹⁴ before use.

Polymerization was carried out in a glass manifold purged with high purity (above 99.96%) nitrogen or argon gas. The gas was purified after passing through a column of molecular sieves (4 Å) and a "BTS" (from Fluka) catalytic oxygen trap. All other glasswares were dried in an oven (130°C) overnight, and the reactor/manifold system went through a few cycles of vacuum-inert gas pumping before the reactions. The solvent, monomer, and initiator were all transferred using syringes.

The solvent used for polymerization was THF. The solvent was first distilled over copper(I) chloride to remove peroxide and then refluxed with sodium metal under nitrogen for 24 h. An indicator, benzophenone, was added for indication of dryness. Freshly distilled THF was used for each polymerization batch. In a typical polymerization reaction, 50 mL of dried THF was first injected into the reaction flask. A few drops of the initiator was added to titrate the solvent from all remaining trace amount of impurities. Then 0.5 mL (for a 1 M initiator) of initiator was injected into the solvent, and the reaction temperature was lowered to -78°C using an acetone-dry ice bath. VSO (5 mL) was added last under constant stirring. The reacting solution turned greenish-yellow immediately, indicating the presence of "living" α -lithio sulfinyl carbanion. The reaction was terminated using degassed methanol after a 30-min reaction time. The poly(phenyl vinyl sulfoxide) (PVSO) was collected by precipitation with diethyl ether. It was purified by further precipitation and followed by vacuum drying to a white powder. The molecular weight (MW) of the polymers was determined by gel permeation chromatography (GPC) and viscosity measurement. Since PVSO is unstable at room temperature, it was kept below -20°C under a nitrogen blanket before further reaction or analysis.

Oxidation, Elimination, and Doping. Poly(phenyl vinyl sulfoxide) was oxidized to random copolymers of phenyl vinyl sulfoxide and phenyl vinyl sulfone using 55% *m*-chloroperbenzoic acid (mCPBA). Different amounts of mCPBA were first dissolved in MeCl and were then added slowly to 5–10% MeCl polymer solutions under vigorous stirring. The copolymers were each purified by reprecipitation twice using THF and diethyl ether followed by vacuum drying. For complete oxidation to poly(phenyl vinyl sulfone) (PVSO_2), an excessive amount of 30% hydrogen peroxide (up to 20 M) in acetic acid was used. The completely oxidized polymers eventually precipitated out from the reaction solution after 24 h. The PVSO_2 was collected from water and purified by another precipitation using chloroform and methanol. The extents of oxidation were characterized by IR spectroscopy.

Predried powders of PVSO and its oxidized copolymers were die-cast into pellets of 0.5 in. in diameter using a KBr sample die and a 12-ton lab press. The pellets obtained were clear smooth films with thicknesses in the range $(1\text{--}3) \times 10^{-3}$ in. In the elimination step, the pellet was first placed in a small glass reactor connected to a vacuum source (10^{-3} to 10^{-4} mmHg) fitted with a cold trap. The reactor was then placed in a furnace equipped with a temperature controller (Shimadzu Model SR24-1Y-000). The sample was heated from room temperature to the selected elimination temperature at a rate of $1^\circ\text{C}/\text{min}$ and was then kept at the maximum temperature for 4 h. The sample color changed gradually from light yellow to reddish-brown or black depending on the oxidation level. The optimal elimination temperature was found to be 150°C . After the reactor has been cooled to room temperature, the reactor was filled with dried inert gas. Then about 10 mL of degassed toluene (sufficient to cover the sample) was added to the eliminated pellet (now appeared porous) in order to extract all the remaining elimination side products, benzenesulfonic acid (PhSO_3H) and its dehydrated products. After 2 h, the solvent was withdrawn and a fresh batch of toluene was added to repeat the washing process. Finally, the pellet was

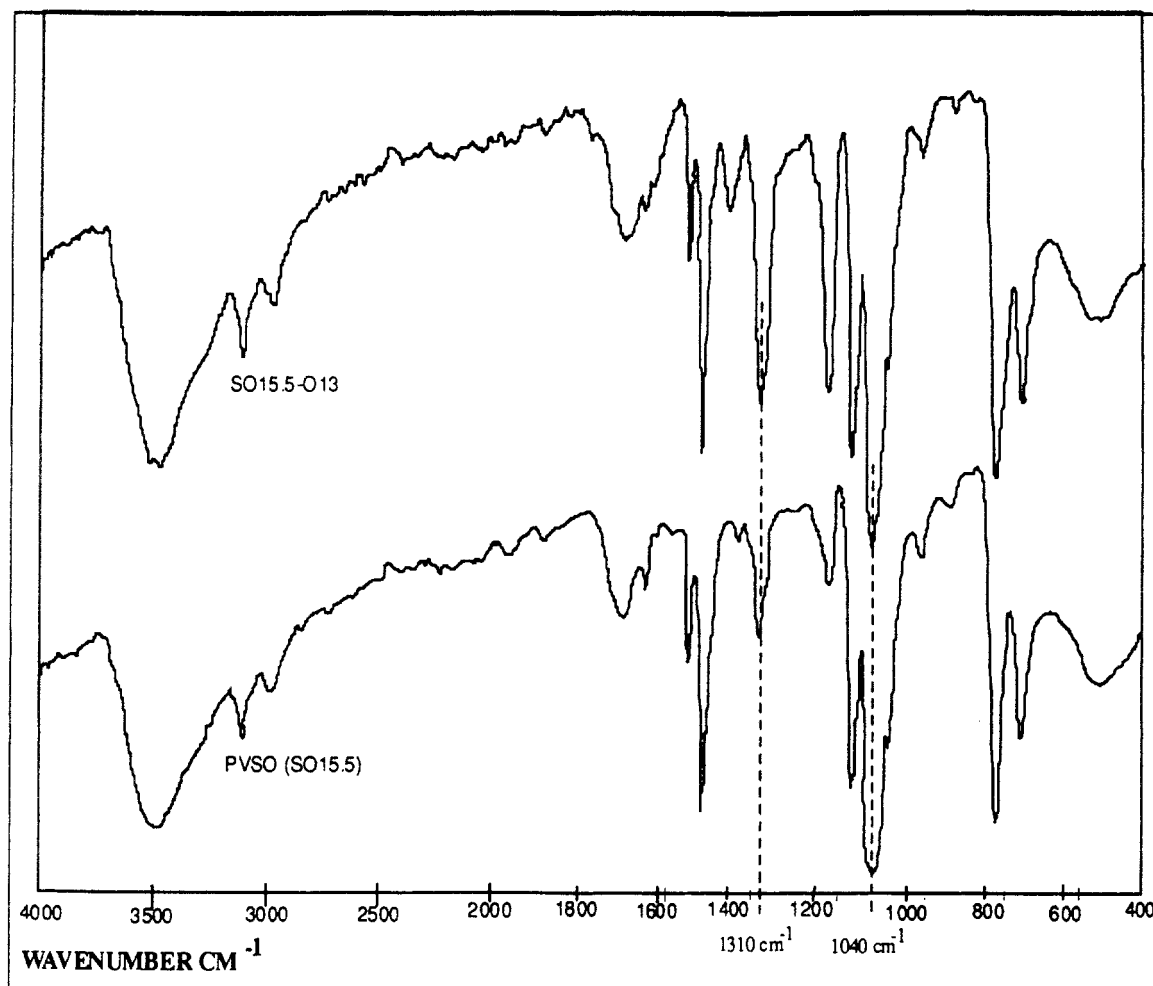


Figure 2. Infrared spectrum of a poly(phenyl vinyl sulfoxide) homopolymer (SO15.5) and its oxidized copolymer (SO15.5-O13). The absorption regions used for the calculation of degree of oxidation are indicated by the dashed lines.

dried under vacuum. Since polyacetylene is highly reactive toward air, the sample was handled under inert gas for all analysis except for electrical measurement which will be performed under ambient conditions. The extent of elimination was determined by a gravimetric method.

Polyacetylene (p-PA) obtained from the elimination of PVSO homopolymer was doped using either a n- or p-type dopant including iodine, concentrated sulfuric acid (97%), concentrated perchloric acid (70%), and 1 M sodium naphthalide THF solution. Except for iodine, the eliminated pellet was doped by immersing into the doping solution under inert gas atmosphere. After hours, the liquid was withdrawn and the sample dried in vacuum. A gas-phase doping method was used for iodine. The polymer pellet was first placed in a glass reactor filled with inert gas together with some iodine crystals. The reactor temperature was then lowered to the boiling point of liquid nitrogen before evacuating. The reactor was then isolated from the vacuum source before returning to room temperature for 24 h. For the partially oxidized copolymers and the uneliminated PVSO and PVSO₂ samples, a higher doping temperature at 50 °C was adopted for the purpose of a higher dopant diffusion rate. All samples were doped to saturation, and the doping level was determined by gravimetric method.

Characterization. ¹H-NMR and infrared (IR) spectroscopy were employed for routine analysis of the monomers, homopolymers, and copolymers. The extent of oxidation for PVSO was determined by comparing their IR absorptivities at 1040 cm⁻¹ (S=O stretching) and 1310 cm⁻¹ (O=S=O stretching). The concentration of sulfoxide and sulfone in the copolymer was then derived from a calibration curve constructed from mixing purified PVSO with VSO₂ monomer at different weight ratios. A typical IR spectrum of PVSO and its partially oxidized product is shown in Figure 2. For liquid samples, a sodium chloride cell was used; for solid samples, they were either in the format of a KBr pellet or polymer thin film. All IR spectra were recorded on a Hitachi

150-20 or a Bio-rad FTS-45 FTIR spectrophotometer. ¹H-NMR spectra were recorded on a JEOL JNM-PMX 60SI NMR using CDCl₃ as solvent and TMS as internal standard.

The intrinsic viscosity of the PVSO homopolymers and a series of polystyrene molecular weight standards (Polymer Laboratories, MW = 10 200, 28 000, 87 000, 410 000) were determined with a Cannon-Fenske capillary viscometer at 25 °C using THF as solvent. GPC measurement for the polymer samples was carried out in a Waters Model 590 HPLC equipped with a Polymer Laboratories column (PL gel- μ mixed) and a refractive index detector. The eluent employed was degassed and microfiltered THF. A universal calibration curve was constructed by plotting the product of the intrinsic viscosity ($[\eta]$) and the molecular weight (MW) of the polystyrene standards against their retention times (t), i.e. $[\eta]MW$ vs t . The molecular weight of the PVSO polymers was calculated on the basis of the universal calibration curve.

Thermal analyses were performed on a Shimadzu DSC-50 differential scanning calorimeter interfaced to a personal computer and a Shimadzu TGA-40 thermogravimetric analyzer. Samples in powder form were used whenever available, and all runs were carried out under nitrogen purge. The heating rate was 5 °C/min from room temperature to 600 to 800 °C for TGA and 20 °C/min from room temperature to 200 °C for DSC studies. Electrical property measurements were effected on a GenRad 1693 RLC digi-bridge. Volume conductivity was measured using a knife-edge four-point probe test fixture, and the dissipation factor was obtained by the parallel plate method. All metallic contacting points were gold-plated. The digi-bridge was set to constant current mode, and the testing frequencies were 0.0117, 0.1, 1, 10, and 100 kHz. Results from the lowest testing frequency at 11.7 Hz were compared to dc conductivity from other studies. In order to avoid the possibility of dopant loss in air, electrical measurement for all doped samples was performed as soon as the sample was exposed to air.

Table I. Anionic Polymerization of VSO Using Various Initiators in THF at -78°C

sample	initiator	amt added (mmol)		theo \bar{M}_n	exp			[η] (dL/g)
		initiator	VSO monomer		\bar{M}_n	\bar{M}_w	\bar{M}_w/\bar{M}_n	
SO15.2	1 M TPMLi	0.3650	32.85	13 700	15 200	18 400	1.21	0.059 59
SO21.2	1 M TPMLi	0.5475	49.27	20 500	21 200	25 600	1.21	0.087 12
SO29.1	1 M TPMLi	0.7299	65.69	27 400	29 100	37 800	1.30	0.124 9
SO14.5	1 M DPMLi	0.3650	32.85	13 700	14 500	18 700	1.29	0.058 71
SO13.8	1.2 M LiNaph	0.7300	32.85	13 700	13 800	18 900	1.37	0.057 52
	1.2 M PhLi	0.3650	32.85	13 700				
	1.5 M <i>n</i> -BuLi	0.3650	32.85	13 700				

Results and Discussion

Polymer Preparation and Characterization. For the five anionic initiators tried for the polymerization of VSO, only the electron-transfer initiator (i.e. LiNaph) and the delocalized carbanion initiators (i.e. TPMLi and DPMLi) were able to polymerize VSO successfully as suggested earlier.¹⁰ The molecular weight of the polymers determined from GPC and intrinsic viscosity measurement are listed in Table I. The number-average molecular weight (\bar{M}_n) of PVSO prepared is in the range 13 000–30 000. Higher MW polymers were not obtained due to the presence of impurities in the reaction medium as well as side reactions that may terminate the “living” anions. This is manifested by the \bar{M}_n measured in general which is slightly higher than the theoretically predicted value. One possible impurity is benzenesulfenic acid (PhSOH). It is a decomposition product of VSO and may have retained in the distilled monomer. The polydispersity index for the anionic prepared polymers, in most cases, is below 1.3. The relatively broad MW is the result of side reactions such as base-promoted elimination of PVSO by the growing carbanion.¹⁰ Since the delocalized carbanion initiators produced polymers with the lowest polydispersity, all PVSO polymers used in the subsequent study were prepared from TPMLi. The PVSO polymers are labeled SOXX.X, in which XX.X is the \bar{M}_n of the polymer in units of thousand. The density of the neat polymers was determined by the displacement method in *n*-heptane using a polymer thin film solvent cast on a glass slide. The relative density was found to be 1.382 g cm⁻³ for PVSO and 1.244 g cm⁻³ for PVSO₂.

Thermal Properties. The glass transition behavior for PVSO (SO15.5) was not observed from room temperature to 200 °C using DSC scanning at 20 °C/min. Instead, a PVSO elimination exotherm with an onset temperature at 130 °C was detected. Although the glass transition temperature (T_g) of PVSO is expected (from its chemical structure) to be lower than 130 °C, the T_g was not found. This is due to elimination of PVSO, which has been reported to initiate even at room temperature and increase rapidly with temperature.¹¹ The formation of a rigid unsaturated backbone structure shifted the T_g to a higher temperature, and the T_g was eventually masked by the elimination exotherm. In addition, a DSC scan of a SO15.5 sample already eliminated at 150 °C for 4 h also did not show the *cis-trans* isomerization transition for PA which was reported to occur at 145 °C.¹ As a result, all p-PA obtained using the same elimination condition can be considered to have a *trans* conformation. For a completely oxidized PVSO₂, a T_g was found at 128 °C (midpoint). The absence of any exotherm also indicated the sulfone-based polymer is thermally stable and would not undergo any elimination transformation process up to 200 °C.

Two distinct weight loss steps were observed for a PVSO (SO15.5) using thermogravimetric analysis. The onset temperature for the first degradation step was found at 135 °C, and its maximum weight loss occurred at about 195 °C. This weight loss step is assigned to the elimination

of PhSOH from PVSO. For 100% elimination, a total weight loss of 83% was calculated. Instead, a weight loss of only about 80% was obtained for the homopolymer. The difference suggested a portion of the phenyl sulfoxide groups either has not eliminated or other side reactions have occurred. The presence of an α -hydrogen adjacent to the sulfoxide moiety is required for the continuation of propagating the zipperlike cyclic sigmatropic elimination reaction.¹⁰ Kanga et al.^{10,11} have reported a maximum weight loss temperature at 200 °C, which is substantially higher than the peak temperature of the exotherm at 146 °C using a DSC. The origin of the discrepancy laid with the different methods used. TGA measured the temperature at which diffusion and evaporation of the elimination side product attained a maximum at ca. 200 °C, while the actual exothermic elimination reaction reached a maximum at ca. 150 °C according to the DSC.

The second degradation step for PVSO occurred at around 450 °C with a 5% total weight loss. This is the degradation temperature range of polyacetylene, as reported earlier.¹¹ For a sample that has been eliminated at 150 °C for 4 h, only the degradation step associated with polyacetylene was detected. The degradation onset temperature for an already eliminated p-PA was found at 410 °C with the maximum weight loss temperature at 450 °C and a total weight loss of 45%. For a fully oxidized PVSO₂, only a single degradation step was detected. The onset temperature was found at 240 °C with the maximum weight loss temperature at 350 °C and a total weight loss of 38%. The single step degradation for PVSO₂ also concluded that the polymer is thermally stable compared to PVSO and it degrades via a mechanism other than elimination of the pendant groups. For a partially oxidized PVSO, i.e. a copolymer of VSO and VSO₂, all three weight loss steps were observed. The onset of the PVSO₂ degradation overlapped with the elimination step of PVSO. Therefore the degree of elimination and the percentage of sulfone group in the copolymer cannot be calculated accurately using this weight loss method. Instead, an IR spectroscopic technique together with a calibration curve was used for the calculation of the sulfone moiety in a partially oxidized PVSO copolymer.

Electrical Properties of the Homopolymer. Both PVSO and PVSO₂ were insulative before elimination and doping. The volume conductivity of PVSO measured at the lowest test frequency (11.7 Hz) was found to be in the range of 6×10^{-9} S/cm. This relatively high conductivity for the undoped PVSO may have been caused by absorbed moisture as well as ionic effects from a small quantity of elimination side product trapped in the polymer matrix. The conductivity of PVSO and PVSO₂ both increased in magnitude while their dissipation factor decreased with increase in measuring frequency.

Even before elimination, PVSO absorbed a large quantity of iodine by the gas-phase doping method. The weight uptake was approximately 1.45 iodine atoms per PVSO repeating unit. The absorption of iodine in the uneliminated PVSO is probably a result of specific interaction

between the unsaturated phenyl ring and iodine. The conductivity for the iodine doped PVSO was in the range of 7×10^{-5} S/cm (11.7 Hz). After the sample was subjected to a direct current for 20 min, the conductivity reduced to 4×10^{-6} S/cm, indicating removal of ionic conduction. The conductivity increased with the measuring frequency and reached a magnitude of 10^{-4} S/cm at 100 kHz. The dissipation factor, however, decreased continuously with the measuring frequency. The origin of this high conductivity is unknown, but similar electrical behavior has been observed for a disordered semiconductor¹⁵ and PA doped with specific dopants at a doping level below the percolation concentration.^{16,17} A variable range hopping mechanism of conduction has been proposed for these systems. The same trends in frequency dependence on conductivity and dielectric constant, however, have also been observed for carbon black filled conducting composites when the volume fraction of the conducting dispersions is small.¹² Interfacial polarization of the two-phase system according to the Maxwell-Wagners-Sillars theory has been proposed to account for the phenomenon. Since it is not known whether the doped PVSO has segregated into regions rich in iodine-phenyl ring complexes, the exact mechanism responsible for the observed conductivity cannot be explained. Similar conducting behavior has also been reported for the ionomer¹⁸ below its T_g and was suggested to be a result of polarization of absorbed water molecules.

The extent for elimination in PVSO was determined according to the sample weight loss after extensively washing with toluene. The ultimate purpose of the extraction was to remove all the remaining benzenesulfenic acid in the polymer matrix. The p-PA pellet after elimination was found to be black in color and has a rather porous structure. The volume percentage of voids was estimated by comparing the density of the eliminated pellet (by direct measurement of the sample volume and weight) with the density of polyacetylene and PVSO. The relative density for *trans*-PA obtained from Shirakawa's method using X-ray crystallography was reported to be 1.13.¹ The maximum amount of voids thus calculated for the eliminated pellet was as high as 70%. The estimation may be in the high end since p-PA obtained from the precursor method would have a lower degree of crystallinity. Density as low as 1.05 has been reported for PA prepared from another precursor method.² This value, however, was not employed here because the degree of elimination and other physical constants are unknown. The void volume fraction (ϕ) was used to correct for the volume conductivity of the eliminated polymer by assuming the sample thickness to be a fraction (i.e. $1 - \phi$) of the value measured using a micrometer. Before doping, the conductivity of an eliminated sample was on the order of 10^{-6} S/cm (11.7 Hz), which is similar to the value reported for a *trans*-polyacetylene.^{1,2}

The optimum conditions for the elimination of PVSO (SO15.5) were obtained by comparing results from five different elimination temperatures ranging from 110 to 200 °C (each for 4 h). The molar percentage of sulfoxide pendant group eliminated was found to increase with the elimination temperature as indicated in Table II. The volume conductivity of the samples after doping with iodine, however, was found to reach a maximum for sample eliminated at 150 °C. At higher elimination temperatures, other forms of defects such as cross-linking of the p-PA chains or homolytic breakage of the sulfur-carbon bond in the sulfoxide group may result.¹⁹ Irrespective of the elimination conditions being chosen, the percentage of

Table II. Effect of Applying Different Elimination Temperatures for 4 h

elimination temp (°C)	% of elimination	doping level, y	conductivity at 11.7 Hz (S/cm)
110	90.53	0.16	3.22×10^{-1}
130	93.17	0.17	1.53
150	95.36	0.16	4.40
170	96.21	0.15	5.62×10^{-1}
200	96.45	0.17	2.11×10^{-1}

elimination was always less than 100%. The optimum elimination temperature at 150 °C was selected for all subsequent studies and the resulting percentage of elimination was in the range of $90 \pm 5\%$. The incompletely eliminated polymer can be considered to be a copolymer of acetylene and the defective groups although not necessarily randomly distributed. Under the relatively mild elimination conditions at 150 °C, all defective groups were assumed to be uneliminated phenyl sulfoxide pendant groups.

In order to identify samples with different elimination efficiencies, the eliminated polymers are denoted by SOXX.X-EZZ, where ZZ represents the molar percentage of phenyl sulfoxide among all sulfoxide groups initially present that has been eliminated. Also, the doping level for the eliminated product is written as (CHD y) x , where y represents the molar ratio of the dopant D to a CH unit. As the elimination process was always less than 100% and the uneliminated phenyl group has some affinity with the iodine dopant, the actual y value per CH unit should be lower than the value reported and depends on the number of phenyl groups remaining in the polymer chain. Compared to the conductivity of iodine doped PA prepared from other precursor methods, they are within the same order of magnitude. The dc conductivity for an iodine doped ($y = 0.27$) PA obtained from the Durham route is 10 S/cm.² The conductivity for a typical iodine doped ($y = 0.4$) *trans*-polyacetylene obtained from Shirakawa's method is higher, in the range of 160 S/cm, due to the orderly crystalline structure.¹

Apart from the chemical structure and morphology of the polymer, the conductivity of a conducting polymer also depends on the nature of the dopant used. The results of p-PA doped with different types of dopant are given in Table III. The p-PA was found to have been successfully doped by either p- or n-type dopant. Samples doped with concentrated sulfuric acid and perchloric acid achieved the highest conductivity (11.7 Hz). These conductivities, however, decreased by 1 order of magnitude, from 10^4 to 10^0 S/cm, after prolonged measurement and exposure to ambient conditions (18–20 °C, 50–60% RH). The loss in conductivity can be a result of a decrease in ionic conductivity and/or loss of dopant in air. Sodium has the smallest overall increase in conductivity because the dopant is highly reactive toward moisture. Among all the dopants tested, iodine was found to have the most stable electrical properties. This is a result of its inertness toward air (both moisture and oxygen), and gas-phase doping provided the highest degree of homogeneity in dopant distribution.

Since all doped p-PA showed a decreasing trend in conductivity after exposure to air (see Table III), the loss of dopant and therefore conductivity was studied by monitoring the time and temperature stability of an iodine doped p-PA sample. The conductivity of a saturation doped sample (SO15.5-E92, $y = 0.31$) was monitored after exposure to air at ambient conditions (18–20 °C, 1 atm and 50–60% RH) for a long time. Both the doping level and conductivity (11.7 Hz) decreased rapidly within the

Table III. Conductivity of Eliminated PVSO Using Various Doping Agents

PVSO sample ^a	dopant	% of elimination	doping level, y	conductivity at 11.7 Hz (S/cm)		
				time = 0	time = 5 min	time = 1 h
SO15.5	I ₂ ^b	92	0.16	2.8	2.8	2.5
SO15.5	I ₂ ^b	89.1	0.17	1.9	1.7	1.5
SO15.5	H ₂ SO ₄ ^c	88.5	0.23	2.9×10^1	1.1×10^1	1.0×10^1
SO15.5	H ₂ SO ₄ ^c	89.1	0.25	1.7×10^1	9.0	7.0
SO15.5	Na ^d	91.1	0.09	7.1×10^{-3}	2.1×10^{-3}	3.5×10^{-4}
SO15.5	HClO ₄ ^c	83.0	0.20	3.5	1.0	8.5×10^{-1}
SO15.5	HClO ₄ ^c	91.2	0.22	2.1×10^1	1.2×10^1	7.0

^a All samples were eliminated at 150 °C for 4 h. ^b Gas-phase doping. ^c Liquid-phase doping. ^d Doped with 1 M sodium naphthalide in THF solution.

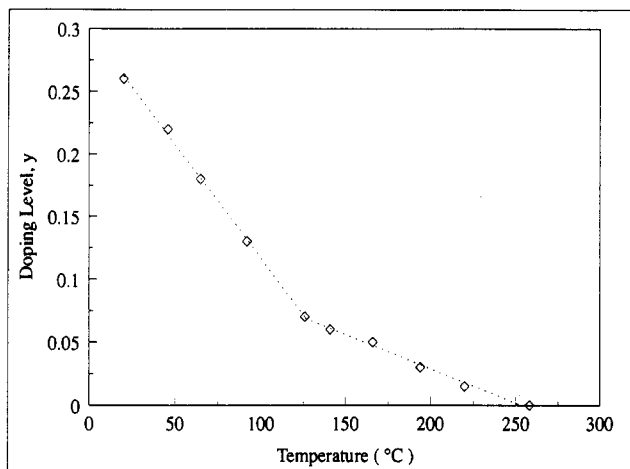


Figure 3. Iodine weight loss for a saturation doped p-PA (SO15.5-E91, $y = 0.26$) as a function of temperature measured by TGA at 5 °C/min purged with nitrogen. Two linear regions are extrapolated and shown as the dashed lines.

first hour. They stabilized only after a few hours. The conductivity was eventually dropped by 1 order of magnitude, and the dopant y value decreased from 0.31 to above 0.1 after 25 h. The dependence of doping level on temperature was measured using a TGA continuously purged with nitrogen. The sample (SO15.5-E91, $y = 0.26$) has a volume conductivity of 2.3 S/cm (11.7 Hz) before the heat treatment. After heating to 260 °C at a rate of 1 °C/min, the doping level reduced to $y = 0.002$ and the conductivity measured was 2.3×10^{-3} S/cm. The change in doping level (y) with temperature is shown in Figure 3. A discontinuity in the slope was detected at 125 °C. The dopant rate loss was 1.9 mmol/°C from room temperature to 125 °C and 0.41 mmol/°C from 125 to 260 °C. The change in iodine rate loss is probably due to the existence of two types of counterions I₅⁻ and I₃⁻. Studies performed by ¹²⁹I Mössbauer spectroscopy^{2,4} have shown that I₅⁻ ions are predominant at high doping levels (at low temperature) while the concentration of I₃⁻ ions increases as the doping level decreased (at high temperature). The relative stability of the counterions is in the order I₅⁻ > I₃⁻ > I⁻.

Since the PVSO elimination was always less than complete, the effects due to the presence of a small number of uneliminated pendant groups on its electrical properties can be studied. At this low defect concentration, the quantity of the uneliminated side group can be readily controlled by adjusting the elimination conditions alone. Lowering the elimination temperature as well as shortening the time for elimination yielded five p-PA samples (SO15.5-EZZ) with extent of elimination from 90 to 95%. Since the elimination process has been described as a concerted process, the uneliminated groups were not necessarily distributed randomly. But from the continuous color change upon heating and a lower conductivity for sample

eliminated under milder conditions, some distributions on the remaining phenyl sulfoxide groups were expected. Distribution of the uneliminated groups is suggested to depend on kinks in the polymer chain conformation and therefore the availability of α -hydrogen, adjacent to the sulfoxide moiety, which is necessary for the completion of the cyclic sigmatropic elimination process.

The doping level, conductivity, and four other calculated variables based on the chemistry of the eliminated polymer chain are given in Table IV. The number percentage of defects is the sum of all structures that will hamper an intrachain charge transport process, such as the uneliminated sulfoxide groups and the polymer chain ends. The volume and weight fractions of acetylene units (corrected for void fraction) are the molar ratios of acetylene repeating units in the eliminated polymer chains derived from the density of the homopolymers. The mean conjugation length (MCL) is calculated by assuming the uneliminated defects were distributed randomly on the polymer backbone. It is equal to $(\bar{X}_n - S)/(S + 1)$, where \bar{X}_n is the number-average number of repeating units and S is the number of uneliminated sulfoxide groups. Details on the calculation can be found in ref 20.

In Figure 4a–d, the number percentage of nonconductive defects, the volume and weight fraction of acetylene units, and the MCL for the incompletely eliminated p-PA are plotted against their volume conductivities (11.7 Hz), respectively. Following Schäfer-Siebert et al.,²¹ a linear relationship was used to fit the data in a semilog plot of conductivity versus percentage of defects (see Figure 4a). The empirical equation obtained was

$$\sigma(d) = \sigma(0)e^{-0.52d}$$

where d is the total number percentage of defects and $\sigma(d)$ and $\sigma(0)$ are the conductivity at d and 0% of defects. The conductivity extrapolated to zero percentage of defects is 110 S/cm and the exponential constant -0.52 is slightly higher than the value -0.55 obtained by Schäfer-Siebert et al. The difference can be the result of a number of factors. (i) The elimination process was not completely random since it has been described to have a "zipper" mechanism;¹¹ (ii) The doping level varied slightly from sample to sample; (iii) The effectiveness of the defects in interrupting the delocalized π -electron may be different. Also, chain ends were not included as defects in the previous calculation.²¹

Similar exponential relationships have been obtained for the other variables (see Figure 4b–d). The conductivity extrapolated to 100% by volume (v) and weight (w) ratio of acetylene was 105 and 135 S/cm, respectively, using the empirical equations

$$\sigma(v) = \sigma(100)e^{0.17(v-100)}$$

and

$$\sigma(w) = \sigma(100)e^{0.17(w-100)}$$

At zero volume and weight percent of conducting segment,

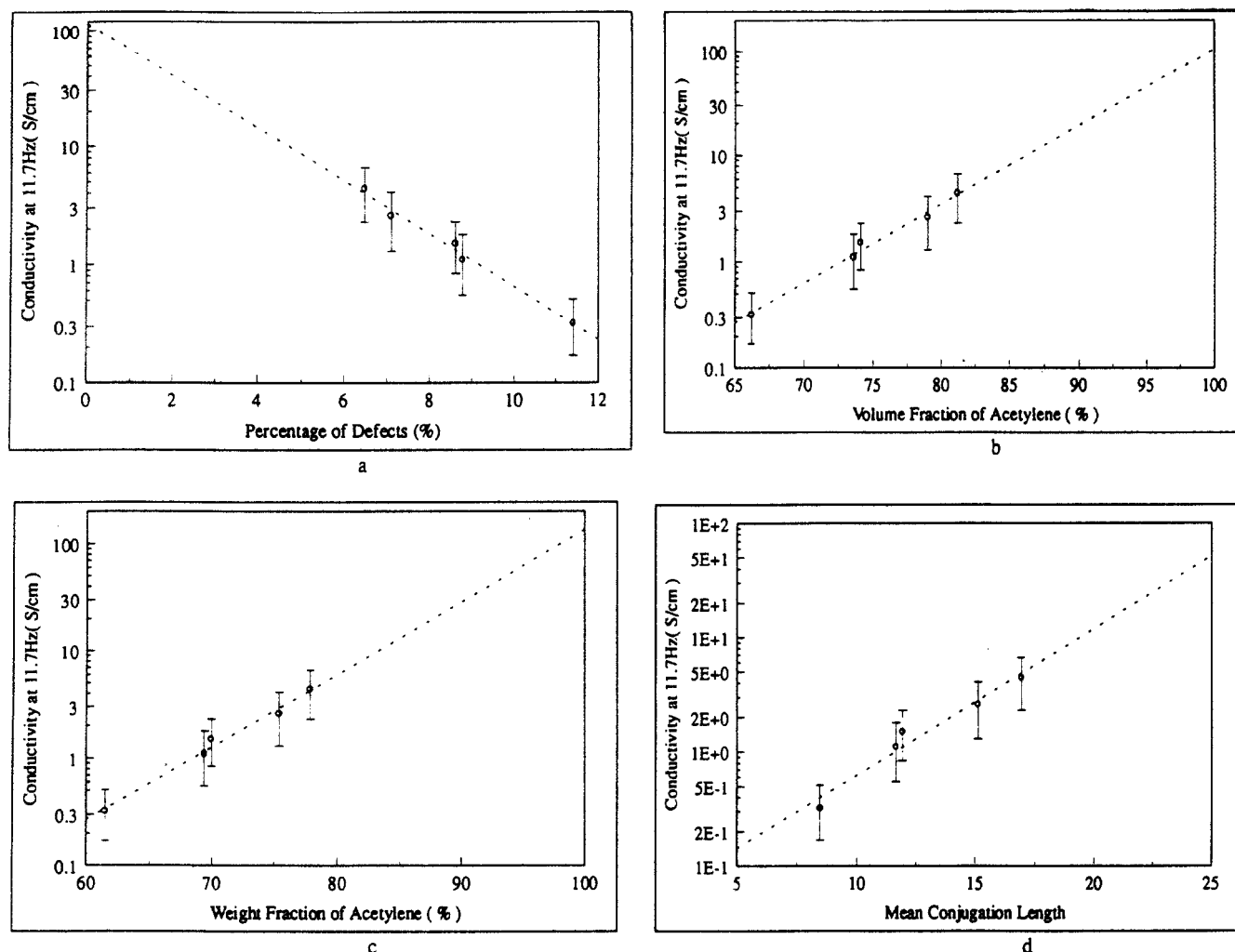


Figure 4. Volume conductivity for a series of iodine doped and incompletely eliminated PVSO homopolymers measured at 11.7 Hz. The plot is against (a) the number percentage of defects, (b) the volume percentage and (c) weight percentage of acetylene units, and (d) the mean conjugation length. A linear least squares method was used to obtain the dashed lines in the semilog plot.

Table IV. Conductivity of Incompletely Eliminated PVSO as a Function of Different Calculated Variables

sample	elimination condition	doping level, y	no. % of defects	vol. fraction of acetylene (%)	wt fraction of acetylene (%)	mean conjugation length	conductivity at 11.7 Hz (S/cm)
SO15.5-E95	temp = 150 °C, 4 h	0.17	6.48	81.16	77.82	16.95	4.40
SO15.5-E94	temp = 150 °C, 2 h	0.16	7.10	79.00	75.4	15.13	2.60
SO15.5-E93.1	temp = 130 °C, 4 h	0.17	8.62	74.10	69.98	11.93	1.50
SO15.5-E93	temp = 130 °C, 2 h	0.17	8.79	73.59	69.42	11.65	1.10
SO15.5-E90	temp = 110 °C, 2 h	0.16	11.41	66.21	61.48	8.48	3.20×10^{-1}

i.e. $\sigma(0)$, the conductivities extrapolated for the uneliminated polymer were 4.3×10^{-6} and 5.6×10^{-6} S/cm, respectively. These values compared favorably to the experimentally measured data for a doped but uneliminated PVSO.

A MCL of 25 repeating units was determined for polyacetylene prepared from Shirakawa's method using electron nuclear double resonance (ENDOR).²² The conductivity extrapolated to a MCL of 25 units in Figure 4d was found to be 50 S/cm, which is lower than the literature value of 160 S/cm for a crystalline PA. Chien et al.²⁴ has suggested the dc conductivity for an iodine doped PA having 15–20 conjugated unit is 1 S/cm and is within the range predicted in Figure 4d. At the lower end of the MCL spectrum, the conductivity approached 10^{-2} S/cm for a MCL of about 1 which coincided with the value reported for a doped polyisoprene.³ The linearity of this parameter, however, was questionable since a relatively high conductivity will remain if linear extrapolation was extended to 0 MCL. For the four calculated variables, the conductivity extrapolated to the value of an ideal p-PA

approaches the results of polyacetylene prepared from Shirakawa's method rather than from other precursor methods. In order to further examine the validity of these exponential relationships, the number fraction of defects was extended to a higher concentration range by partially oxidizing the PVSO precursor polymer to a copolymer of VSO and VSO₂.

Electrical Properties of Partially Oxidized PVSO. As mentioned earlier in the thermal analysis section, the sulfone pendant group is thermally stable (up to 200 °C). By properly controlling the degree of oxidation for a PVSO, the total number of defects in the resulting p-PA can be extended to a higher percentage range. In this study, PVSO (SO15.2) was selectively oxidized to produce a series of VSO and VSO₂ copolymers with sulfone content ranging from 1.2 to 23 mol %. After elimination, the color of the samples ranges from reddish-brown to black depending on the extent of oxidation. In a partially oxidized copolymer, the overall degree of elimination for the remaining sulfoxide pendant groups is also lower than that for a PVSO homopolymer. This is due to the fact that the

Table V. Conductivity of Oxidized PVSO Copolymer as a Function of Different Calculated Variables

sample	doping level, y	no. % of defects ^a	vol. fraction of acetylene (%)	wt fraction of acetylene (%)	mean conjugation length	conductivity at 11.7 Hz (S/cm)
SO15.2-O1.2-E89	0.61	13.94	59.56	54.84	6.64	1.80×10^{-2}
SO15.2-O1.2-E88	0.56	14.69	57.90	53.12	6.22	1.00×10^{-2}
SO15.2-O4.5-E88	0.54	18.05	50.14	45.82	4.80	1.30×10^{-3}
SO15.2-O4.5-E87	0.61	18.41	49.50	45.18	4.68	9.50×10^{-4}
SO15.5-O6.5-E88	0.61	18.97	47.88	41.20	4.50	6.70×10^{-4}
SO15.5-O6.5-E87	0.59	20.35	45.67	38.62	4.11	2.70×10^{-4}
SO15.2-O7.0-E87	0.62	20.60	45.18	35.61	4.05	2.40×10^{-4}
SO15.2-O7.0-E85	0.63	22.32	42.62	33.25	3.64	1.10×10^{-4}
SO15.5-O13-E91	0.65	22.78	40.47	43.86	3.54	9.00×10^{-5}
SO15.2-O9.6-E85	0.71	24.34	39.28	41.61	3.24	2.00×10^{-5}
SO15.5-O20-E96	0.66	24.49	36.92	37.25	3.21	1.90×10^{-5}
SO15.5-O13-E88	0.69	24.84	37.85	34.58	3.15	1.40×10^{-5}
SO15.2-O11-E85	0.63	26.13	36.73	34.37	2.94	2.10×10^{-5}
SO15.5-O20-E92	0.65	27.78	33.29	30.64	2.69	7.50×10^{-6}
SO15.5-O23-E87	0.74	34.60	26.61	24.16	1.94	5.50×10^{-6}

^a Defects included chain ends, uneliminated phenyl vinyl sulfoxide, and phenyl vinyl sulfone.

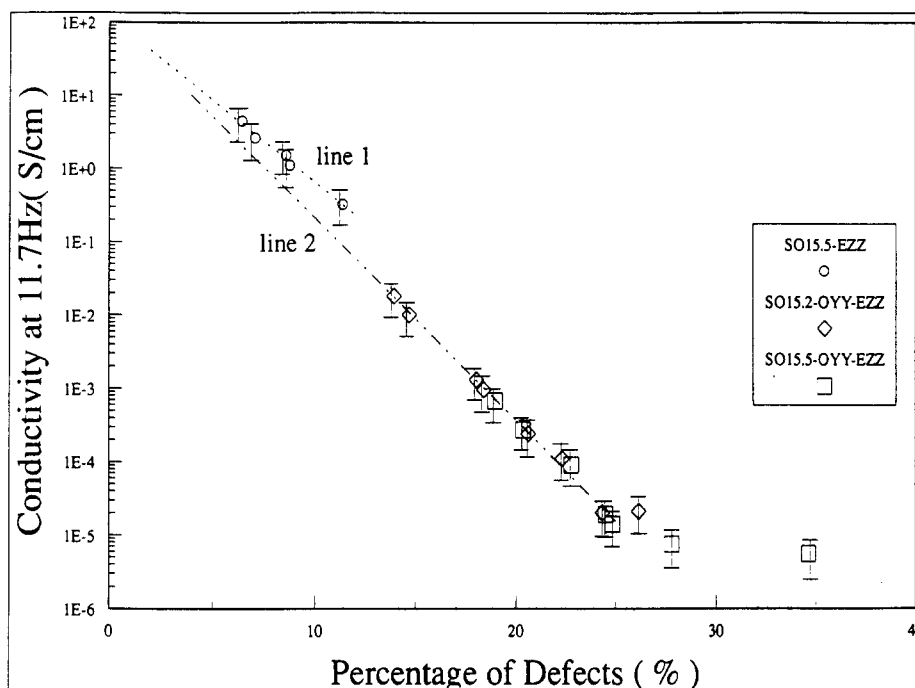


Figure 5. Volume conductivity of doped p-PA copolymers plotted against the total number percentage of defects. Line 1 is extrapolated from data for the incompletely eliminated PVSO homopolymers, and line 2 is extrapolated from the linear region of the partially oxidized copolymers.

elimination that occurred has a zipper mechanism. The presence of a thermally stable sulfone moiety will nevertheless hinder the smooth elimination process, resulting in a higher degree of incomplete elimination. In Table V, the degree of oxidation as well as the conductivity and other variables for the iodine doped copolymers are reported.

The doping level for the copolymer in general is found to be higher than that of the homopolymer. This is partially due to the fact that a higher doping temperatures was adopted. In addition, the strong specific interaction between the uneliminated pendant groups (phenyl sulfone as well as phenyl sulfoxide) also absorbed a large quantity of the dopant. A higher dopant concentration should not affect the comparison of conductivity data with those for the p-PA obtained earlier having a lower doping level. Electrical properties measured for PA doped with halogen were found to reach a steady-state value when y was above 0.2.⁴ For a partially oxidized PVSO, the notation used to represent the copolymer is SOXX.X-OYY-EZZ where YY is the molar percentage of sulfoxide oxidized to sulfone and again ZZ is the molar percentage of sulfoxide eliminated among all sulfoxide groups in the copolymer.

In Figure 5, conductivity measured at 11.7 Hz for the full range of defect percentages is shown. A sigmoidal dependence on conductivity was not obvious. Instead, two linear regions were found for the oxidized and unoxidized products, each with different parameters for the exponential relationship. When the linear portion of the data for the oxidized copolymers (line 2 in Figure 5) is fit with an exponential relationship, the equation becomes

$$\sigma(d) = \sigma(0)e^{-0.64d}$$

The exponent -0.64 is much lower than the -0.52 value reported earlier (line 1). The higher gradient obtained for the oxidized copolymers indicated that the sulfone groups have a higher efficiency in interrupting the delocalized π -electron. The high efficiency can also be due to a less random distribution of defects and pairing of the uneliminated defects (sulfone and sulfoxide) which has occurred. The conductivity extrapolated to zero percentage defects is 125 S/cm, similar to results obtained earlier. Instead of two lines with different slopes, one can also consider a sigmoidal change in which the first

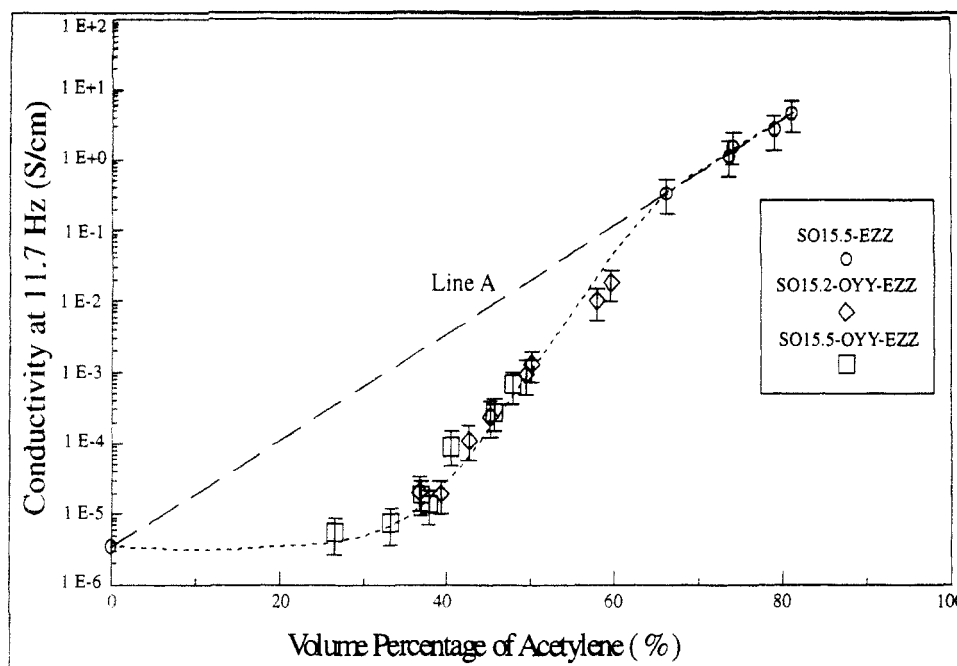


Figure 6. Volume conductivity of doped p-PA copolymers plotted against the volume percentage of acetylene units. Line A is extrapolated from the upper linear region (same in Figure 4b).

discontinuity in the slope occurred at 10–12% defects. This discontinuity suggested a decrease in the efficiency for intrachain charge transport for reasons stated above. The second discontinuity occurred at 25% total defects. The conductivity leveled off at this high defect concentration and approached an asymptotical value at 10^{-6} S/cm. This coincided with the conductivity for a fully doped ($\gamma = 2.9$) but 100% uneliminated PVSO. The relatively constant conductivity at this high defect percentage range suggested the pathway for conduction is through the doped but uneliminated PVSO matrix rather than charge transport amongst isolated conducting segments or regions. At this defect concentration range, the frequency dependent conductivity is similar to a doped but uneliminated PVSO and will be discussed later.

In a separate diagram (Figure 6) on the volume conductivity (11.7 Hz) of the copolymers at different volume percentages of acetylene units, three different linear regions over the full composition range were found. They are for data above 70%, between 35 and 70%, and below 35% volume of acetylene. The exponential relationship applied for data above 70% is reproduced here as line A. Assuming the conducting components were interconnected, line A indicated a continuous increase in conductivity with the volume fraction of conducting element due to an increase in the overall MCL. Deviation of the experimental data below 70% of acetylene from line A, however, indicated the conducting elements were indeed well dispersed and rather isolated. The transition from an interconnected to a discontinued stage is a result of the volume-filling effects of the ever increasing nonconducting elements. The resulting sigmoidal change observed is similar to a conducting filled percolation process, except the conductivity of the conducting filler varied also with the composition. The upper and lower conductivity limits were distinguished by a doped 100% eliminated PVSO, which is on the order of 10^2 S/cm, and a doped but uneliminated PVSO, which is on the order of 10^{-6} S/cm.

A sigmoidal dependence on conductivity was also observed for *cis*-PA and *trans*-PA as a function of iodine dopant concentration.⁴ Since the transition occurred at

very low doping levels ($\gamma = 10^{-1}$ to 10^{-5} of I_3^-), the same phenomenon observed here cannot be caused by the variation of dopant concentration in the different samples. This doping level related percolation phenomenon has been explained by a charge carrier "glass" transition model in which the mobility of the carrier is related to the Coulombic interaction and concentration of the counterions.²³ As the doping level of the various p-PA copolymers studied in this report was at saturation, the system is considered to be above the carrier glass transition temperature with unlimited mobility for the charge carrier. The sigmoidal transition observed is therefore related to the dispersity of the conducting elements rather than to the dopant concentration.

A fluctuation-induced tunneling mechanism model,^{16,24} which is normally applied for conducting composites, can also be invoked here. The model suggested that thermally activated voltage fluctuations between junctions of conducting regions resulted in tunneling of the charge carrier. Instead of a sharp transition usually observed for percolation phenomenon for conducting composites, a broad transition range is observed for this copolymer system. In a previous study on carbon black filled PVC compounds,¹² a broad percolation transition was obtained when the aspect ratio of the filler is high (or low packing efficiency) as well as when the conductivity of the filler is low. The broadening of the transition region for a less conducting filler is due to polarization coupling between the conducting particles and the insulating matrix.¹² In addition, the broad transition observed in Figure 6 can be the result of distribution in conjugation length for a given MCL. At each conjugation length, the conducting segment can also be considered to have a different particle size or shape. The existence of a percolation threshold is also manifested by a maximum in the dielectric loss or dissipation factor measurement. In Figure 7, a broad dissipation factor (1 kHz) curve with a maximum at about 37–38% volume of acetylene is established. This corresponds well to the 35% volume of acetylene at the conducting transition threshold. The relatively large dissipation factor and hence large dielectric constant have also been observed for PA doped with specific dopants.¹⁷

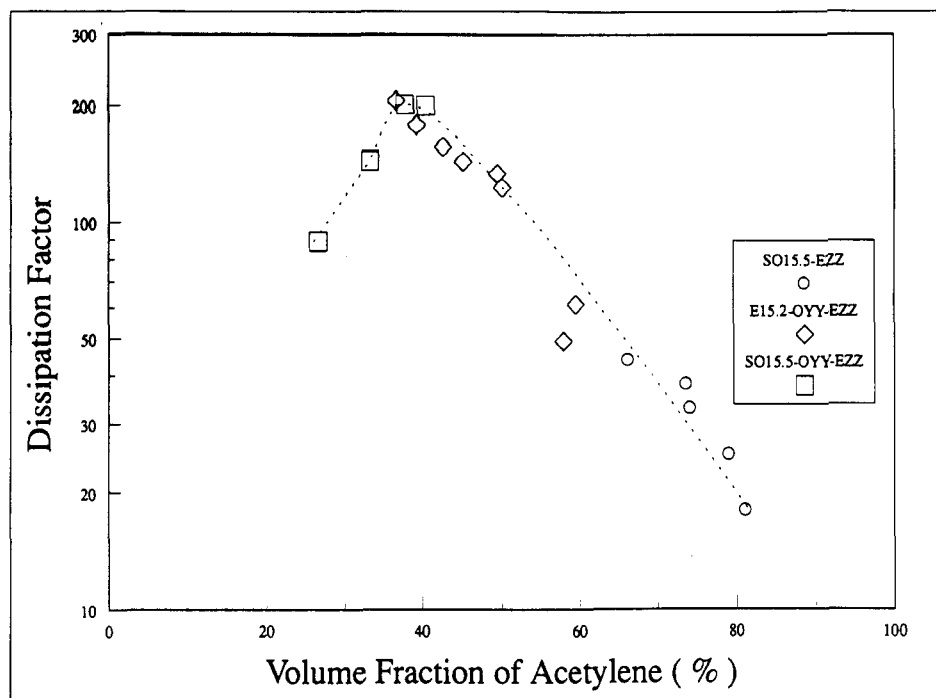


Figure 7. Dissipation factor (at 1 kHz) of doped p-PA copolymers at different volume percentages of acetylene units. The dashed line is an indication of the overall trends only.

On the basis of conducting mechanism proposed for other percolative systems, the charge transport mechanism for the p-PA conducting copolymer will be explained in terms of the volume fraction of the acetylene units. At low acetylene volume fraction, the volume conductivity (11.7 Hz) remained constant up to the percolation threshold at 35%. The conducting domains at this composition range consisted of mostly short conjugated units well dispersed in the semiconducting phenyl ring-iodine matrix. The invariable conductivity suggested the conducting acetylene units did not affect the bulk electrical properties. The conductivity measured is rather a result of charge hopping between the phenyl ring-iodine complexes or polarization of the discrete conducting elements. As the number and size of the conductive element increased, hopping and tunneling between nearby conducting p-PA regions became possible. A broad distribution in tunneling band gap as well as in the inherent conductivity of the conducting segments with different conjugation lengths contributed to the broadness of the transition region. The number of conducting pathway further increased at higher acetylene volume percentage. Finally, the averaged tunneling gap reduced to its critical value at 65% acetylene volume and the conducting polymer achieved its maximum metal-like conductivity. Unlike a conducting filled composite material in which the intrinsic conductivity of the fillers determined the upper conductivity limit, the conductivity continuously increased beyond the percolation composition. This is due to copolymers with higher MCL, and therefore higher conductivity, which are obtained at further decreases of defect contents.

The percolation threshold at 35–38% is slightly higher than the $1/3$ maximum volume fraction predicted by Bruggeman's effective-medium theory when a spherical conductive dispersion is used. The discrepancy can be caused by a number of factors such as not accounting for free volume in the calculation of acetylene volume fraction. The close to $1/3$ threshold volume fraction measured here, however, did not necessarily imply the acetylene units have spherical conformations or geometries. Deviation from the theoretical threshold value can also result when the conducting media are inhomogeneously dispersed or

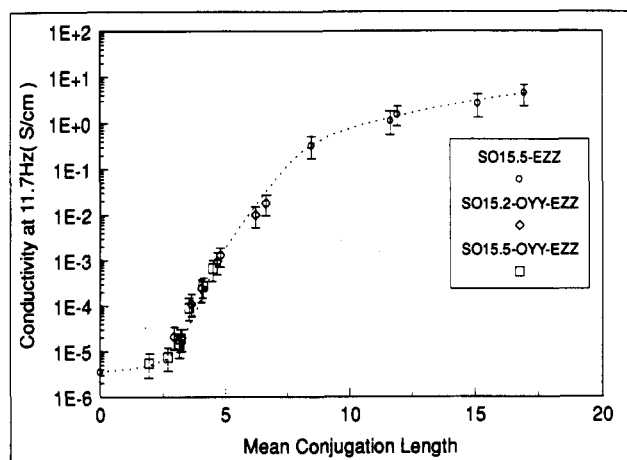


Figure 8. Volume conductivity of doped p-PA copolymers plotted against the mean conjugation length.

phase segregated in the matrix. Phase segregation or filler particles with higher aspect ratios normally depress the threshold to a lower volume fraction. Instead, a high threshold value is obtained for the elongated conjugated conducting segments. This can be explained by assuming the morphology of the copolymer system to have a structure in which the rigid rodlike acetylene units were shielded by the flexible random coil-like uneliminated segments. A similar sigmoidal dependence was obtained when the conductivity data are plotted against the acetylene weight percentage, and the threshold was found at 33–35%. The dependence of the bulk electrical conductivity (11.7 Hz) on MCL is also given in Figure 8. As before, conductivity of the p-PA did not increase continuously with the MCL due to inclusion of nonconducting segments in the system. The conductivity leveled-off at high MCL and reached an asymptotic value at $(1-2) \times 10^1$ S/cm. A percolation threshold at a MCL of ca. 3 was established.

Frequency dependence on the properties of the conducting copolymers was studied by extending the measuring frequency from 11.7 Hz to 100 kHz. The conductivity dependence on the test frequency for a few selected copolymers is given in Figure 9. For copolymers with less

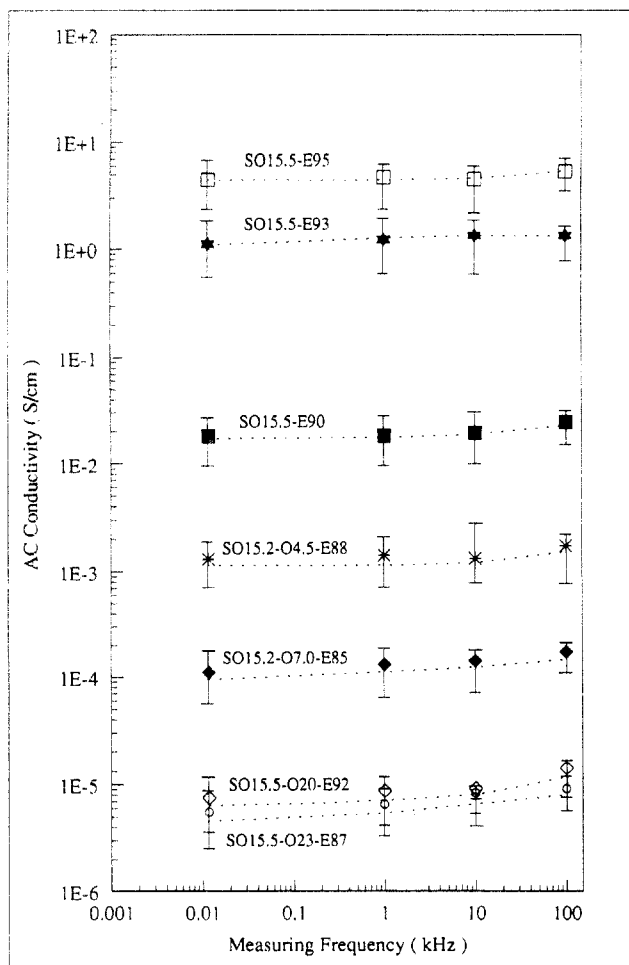


Figure 9. Volume conductivity of the doped p-PA copolymers at different frequency ranges.

than a 65% volume of acetylene, the conductivity increased slightly at a high frequency range which is characteristic of the hopping mechanism of conduction.^{16,17} At higher acetylene volume fractions the conductivity became independent of the test frequency (for the frequency range studied). This is an indication of fully establishment of "metallic" contact between conducting domains. The dissipation factor reduced to approximately zero at around the same composition range. This is due to the conduction process primarily through tunneling or hopping through pathways with the least resistance and therefore with little or no energy loss mechanism.

Conclusion

A chemical method was used to control the number of nonconducting defects in a conducting polymer with known MW and narrow MW distribution. Effects due to disruption of intrachain charge transport by the defects on the bulk conductivity were investigated. The parameters used to quantify the chemical structural changes were the number percentage of defects, the weight and volume percentage of the conducting acetylene units, and the mean conjugation length. An exponential relationship was able to describe changes in conductivity only at highly conducting compositions. Deviation from the relationship, however, occurred when the volume-filling effects of the nonconducting segments became important. The existence of a percolation transition is evidenced from the sigmoidal dependence of conductivity on the volume and weight fractions of the conductive segment as well as a maximum in the dissipation factor measurement. Hopping and tunneling of the charge carrier is suggested to be

the major conduction mechanism as the doping level was above the carrier "glass" transition temperature. Below the threshold composition, the conductivity remained almost constant, indicating no increase in carrier mobility for the highly dispersed conducting elements. Above the percolation threshold, tunneling and hopping between conducting segments led to an increase in the overall conductivity. The broadness of the transition range is suggested to be a result of a broad distribution in conjugation length for each copolymer sample. The averaged tunneling gap decreased continuously and reached a critical value at high acetylene volume fraction. The conductivity of the polymer then approached a final steady-state value, for a particular MCL, and was independent of the measuring frequency. The conducting copolymer system can be compared to a conducting composite in which the conducting filler has a range of conductivities and particle sizes. Further studies on the effects of inhibition of interchain and interdomain charge transport using PVS0 polymer blends and block copolymers will be discussed in a forthcoming study.

Acknowledgment. The work presented in this article was supported by a grant from the UPGC Research Grants Council (RSC) of Hong Kong, Grant No. RSC/90-91/02. The manifold used for anionic polymerization was funded by Grant No. FRG/89-90/I-02. The authors would like to thank Dr. Vincent Cheng for valuable comments on the manuscript.

References and Notes

- (1) Kroschwitz, Jacqueline I., Ed. *Electrical and Electronic Properties of Polymers: A State-of-the-art Compendium*; John Wiley & Sons: New York, 1988.
- (2) Skotheim, T. A., Ed. *Handbook of Conducting Polymers*; Marcel Dekker: New York, 1986; Vols. 1 and 2.
- (3) Thakur, M. *Macromolecules* 1988, 21, 661.
- (4) Chien, James C. W. *Polyacetylene-Chemistry, Physics, and Materials Science*; Academic Press: Orlando, Florida, 1984.
- (5) Ito, T.; Shirakawa, H.; Ikeda, S. *J. Polym. Sci., Polym. Chem. Ed.* 1974, 12, 11.
- (6) Feast, W. J.; Parker, D.; Winter, J. N.; Bott, D. C.; Walker, N. S. *Solid-State Sci.* 1985, 63, 45.
- (7) Gagnon, D. R.; Capistran, J. D.; Karasz, F. E.; Lenz, R. W.; Antoun, S. *Polymer* 1987, 28, 567.
- (8) Bates, Frank S.; Baker, Gregory L. *Macromolecules* 1983, 16, 704.
- (9) Aldissi, M.; Bishop, A. R. *Polymer* 1985, 26, 622.
- (10) Kanga, R. S.; Hogen-Esch, T. E.; Randrianalimanana, E.; Soum, A.; Fontanille, M. *Macromolecules* 1990, 23, 4235.
- (11) Kanga, R. S.; Hogen-Esch, T. E.; Randrianalimanana, E.; Soum, A.; Fontanille, M. *Macromolecules* 1990, 23, 4241.
- (12) Chung, K. T.; Sabo, A.; Pica, A. P. *J. Appl. Phys.* 1982, 53, 6867.
- (13) Paquette, Leo A.; Carr, Richard V. C. *Org. Synth.* 1985, 64, 157.
- (14) Wakefield, Basil J., Ed. *Organolithium Methods*; Wiley Interscience: New York, 1984.
- (15) Abkowitz, M.; Le Comber, P. G.; Spear, W. E. *Commun. Phys.* 1976, 1, 175.
- (16) Tomkiewicz, Y.; Shiren, N. S.; Schultz, T. D.; Thomann, H.; Dalton, L. R.; Zettl, A.; Gruner, G.; Clarke, T. C. *Mol. Cryst. Liq. Cryst.* 1982, 83, 17.
- (17) Sichel, E. K.; Rubner, M. F.; Druy, M. A.; Gittleman, J. I.; Bozowski, S. *Phys. Rev. B* 1984, 29, 6716.
- (18) Hodge, I. M.; Eisenberg, A. *Macromolecules* 1978, 11, 283.
- (19) Kingsbury, C. A.; Cram, D. J. *J. Am. Chem. Soc.* 1960, 82, 1810.
- (20) Tan, K. H. Master in Philosophy dissertation, HK Baptist College, 1992.
- (21) Schäfer-Siebert, D.; Budrowski, C.; Kuzmany, H.; Roth, S. *Solid-State Sci.* 1987, 76, 38.
- (22) Thomann, H.; Dalton, L.; Tomkiewicz, Y.; Shiren, N.; Clarke, T. *Phys. Rev. Lett.* 1983, 50, 533.
- (23) Chien, J. C. W.; Babu, G. N. *J. Chem. Phys.* 1985, 82, 441.
- (24) Sheng, P. *Phys. Rev.* 1980, B21, 2180.